Available online at www.sciencedirect.com

ScienceDirect

Procedia Manufacturing 26 (2018) 993–1002

Procedia MANUFACTURING

www.elsevier.com/locate/procedia

46th SME North American Manufacturing Research Conference, NAMRC 46, Texas, USA

Direct-Ink-Writing of Degradable Carboxymethylcellulose

Alyssa Brandley[a], Robyn Hollfelder[b], Sepehr Nesaei[c], Bernard VanWie[b], Nehal Abu-Lail[b], B. Arda Gozen[c,*]

[a]*Biomedical Engineering Department, Rowan University, Glassboro, NJ, 08028, United States*
[b]*Voiland School of Chemical Engineering and Bioengineering, Washington State University, Pullman,WA , 99164, United States*
[c]*School of Mechanical and Materials Engineering, Washington State University, Pullman,WA , 99164, United States*

* Corresponding author. Tel.: +1-509-335-3214; fax: +1-509-335- 4662
E-mail address: arda.gozen@wsu.edu

Abstract

Additive manufacturing with degradable polymers have recently drawn significant attention due to its promising biomedical applications including artificial tissue engineering, surgical, and orthopedic devices etc. This paper experimentally investigates the direct-ink-writing of one of the widely used degradable polymers, carboxymethlycellulose. Through printing and geometric characterization of simple test structures, effect of ink concentration, substrate material and direct-ink-writing process parameters including printing pressure, printing speed and nozzle substrate distance on the process outcome is studied. Preliminary findings on printing of micro-scale structures using nozzles as small as 10 μm in diameter are also presented.

Peer 46th SME North American Manufacturing Research Conference.

Keywords: Micro-additive manufacturing; biodegradable; hydrogels; micro-extrusion; 3D-printing

1. Introduction

Biodegradable polymers have been widely used in a myriad of applications including surgical, implanted and orthopedic devices, drug delivery systems, artificial tissue engineering and food packaging[1,2]. The importance of such applications directly involving human health brought the need for accurate and robust manufacturing technologies for processing biodegradable polymers. Conventional polymer processing methods have been successfully used for such materials in the past decades. More recently, emergence of biomedical device technologies requiring complex, multi-material and personalized parts with micron-level feature sizes, led to increased research and technological investment in the additive manufacturing with biodegradable polymers.

2351-9789
Peer-review under responsibility of the scientific committee of the 46th SME North American Manufacturing Research Conference.
10.1016/j.promfg.2018.07.130

Various commonly used polymer additive manufacturing techniques have been utilized for biodegradable materials. These methods include, powder bed processing methods such as selective laser sintering and melting [3,4] and binder jetting [5], vat-photopolymerization methods such stereolithography [6] and extrusion-based methods such as fused-deposition modelling [7] and direct-ink-writing (DIW) [8]. Primary application of the additively manufactured parts have been the artificial tissue scaffolds [9] which are complex porous structures that are implanted in the patients' body and facilitate the tissue growth in a particular geometry by providing mechanical support. Among these methods, powder and photopolymerization based ones provide high accuracy and resolution, however lack design and material flexibility: Powder-based methods require the feedstock to in a fine powder form, whereas the photopolymerization methods requires the polymer to be synthesized as photocurable. This limits the usable set of materials, particularly composites including bio-materials such as high density living cell aggregates, growth factors, micro-carriers and decellularized matrix components which are critical for target applications. Furthermore, both types of methods are significantly limited in multi-material implementations and usually are costly [10]. Extrusion-based methods mitigate such issues owing to its top-down nature and ease of multi-material implementations. The low-cost FDM approach is limited to thermoplastic polymers and require high temperature processing and thus cannot be used for processing of polymer composites including biomaterials that are sensitive to temperature. On the other hand, DIW, allows for room temperature processing and capable of processing a wide range of polymer composite "inks", combining biodegradable polymer matrices with additives such as micro-nano-particles [11], living cells [12] and growth factors [13], allowing high level of customization for many biomedical applications. Due to these factors, DIW is considered as the state-of-the art "bioprinting" method, leading to emergence of numerous commercial DIW-based bioprinters in the recent years.

DIW, in general, is an additive manufacturing technique used for highly viscoelastic materials. The research on the DIW processes to date primarily focused on the non-Newtonian shear flow of the inks during their dispensing through the millimeter to micron-scale nozzles[14], effect of their viscoelasticity on the printed structure geometry [15] and capillary effects of the ink spreading and wetting of the substrate surface [16]. Authors' recent work demonstrated the effect of the viscoelasticity on the flow of the inks and the underlying deposition mechanisms during DIW, which can be anywhere between pure extrusion and pure fiber drawing depending on the process and material parameters [17].

During DIW of biodegradable polymers, the inks are usually prepared in the form of concentrated water solutions of the polymers that gellate through water loss or another cross-linking process such as UV-curing [18]. The functional biomaterials are suspended in the hydrogels, and deposited along with the inks during the printing process. DIW of variety of natural and synthetic hydrogels have been demonstrated in the literature [19] towards fabrication of tissue scaffolds. Most of these studies focused on the direct evaluation of the functionality of these scaffolds in regards to biodegradation and cell viability during in-vivo or in-vitro cell culture while the manufacturing science focus on these processes are generally lacking. Particularly, there is only a few recent studies investigated the effect of material and process parameters on the ink-flow and printed structure geometry[20].

This paper presents an analysis of the DIW process using concentrated sodium carboxymethyl cellulose (CMC) inks. CMC is a water dissolvable ether, derived from naturally abundant and biodegradable cellulose through its reaction with sodium monochloroacetate in an alkaline medium [21]. CMC solutions have been widely used in food industry, in detergents and soaps, resin emulsion paints, adhesives and printing inks. More recently it has been utilized for fabrication of microneedles in intradermal drug delivery [22,23]. In this work, simple test structures are printed using nozzles as small as 50 μm diameter, under various material and process conditions and the corresponding DIW outcomes have been studied. Particularly, the effect of ink concentration, substrate surface, printing speed, distance and input pressure on the ink flow rate and the printed geometry are investigated. Some qualitative observations is also presented regarding the printing of CMC inks using ultra-fine nozzles as small as 10 μm diameter.

2. Materials and Methods

2.1. CMC Ink Preparation

Inks were obtained by dissolving sodium CMC

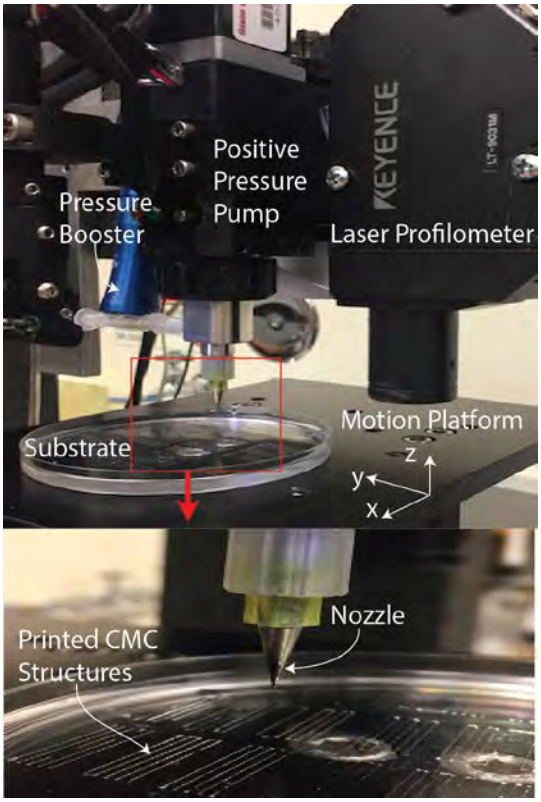

Fig. 1. The custom DIW system

(90kDa molecular weight, Sigma Aldrich) powder in dionized water in two concentrations of 30 and 40% w/w. To obtain these highly concentrated inks, a 15% w/w solution was first prepared by mixing at 300 rpm using a high speed homogenizer (Cole-Parmer Compact Digital Mixer System, 50 to 2500 rpm, 115 VAC) for 3-5 hours until a homogenous solution is obtained. To reach the final concentration, the base ink was kept in a vacuum oven (Lindberg Blue M ThermoScientific) at 55ºC temperature and 25 mmHg vacuum to evaporate water at an approximate rate of 1 mL/hour. During this process, the ink was removed from the oven occasionally and mixed at the high speed mixer for 5 min to maintain homogeneity. For printing, the inks were loaded in 5cc syringe cartridges (Nordson EFD) and centrifuged at 800 rpm for 2 minutes for air bubble removal.

2.2. Rheological characterization of the CMC Inks

The ink rheology was characterized using a strain controlled rheometer (TA Instruments, ARES-G2) through oscillatory frequency and amplitude sweep experiments on a parallel plate setup (8 mm plate diameter). In the frequency sweep tests, the behavior of the inks under varying shear rates were characterized by varying the oscillation frequency at constant oscillation amplitude to understand the shear thinning characteristics of the inks. In the amplitude sweep test, the shear rate is varied through varying the oscillation amplitude by keeping the frequency constant to understand the viscoelastic nature of the inks by observing the variation of their viscous and elastic moduli.

2.3. DIW system and parameters used

A custom made DIW system with integrated profilometry capability pictured in Fig 1 is used for the printing experiments. This system consists of a three axis motion system (Aerotech ANT180-ANT130 stages) having sub-micron accuracy within a working space of 210 mm x 160 mm x 110 mm. A positive pressure pump (Nscrypt Smart Pump Gen 1) is used to regulate the dispensing process. The inks were supplied to this pump through a pressure booster (Nordson EFD HP5cc) which mechanically amplifies the air pressure supplied to it by a factor of four as its piston pushes the ink out of the syringe cartridge into the pump. The pump controls the ink flow through a needle valve that can be positioned with 10 µm accuracy. Two types of nozzles have been used at the pump outlet: For the quantitative analyses, a conical brass nozzle with 50 µm nominal diameter (Fisnar Micro-S Precision Micro Bore Nozzle), for ultra-fine nozzle printing, glass capillaries with 30 and 10 µm diameters were (World Precision Instruments, Pre-Pulled Glass Pipettes). The geometry of the printed structures were measured using a laser profilometer (Keyence LT9031M).

We designed our experiments using a limited set of parameters to preliminarily observe several deposition mechanisms and effect of the process and materials on such mechanisms. For each printing experiment, lines of 15 mm length is printed using either the 30 or 40% inks. These concentrations are selected with respect to their flow behavior through the nozzles: lower concentration inks formed a pendant drop at the nozzle exit, indicating the flow behavior dominated by capillarity. At 30%, a clear filament formation is observed, indicating the prominence of the viscoelasticity that is favorable for printing. For concentrations higher than 40%, rapid ink drying at the

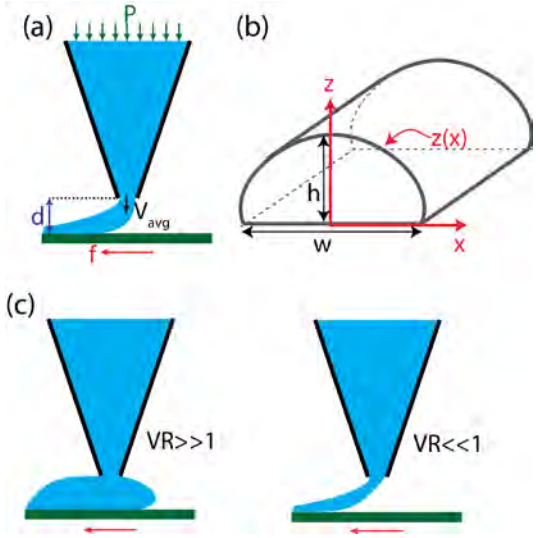

Fig. 2. (a) DIW process parameters, (b) Analysis parameters, (c) Two different deposition mechanisms during DIW

nozzle led to frequent clogging, preventing efficient experimentation.

The process parameters varied in our study are schematically described in Fig 2(a) and include printing pressure (P), nozzle-substrate distance (d) and printing speed (f). Three levels of printing pressure (193, 386 and 579 kPa) was used for each type of ink. Pressures lower than 193 kPa did not produce continuous flow for any of the selected ink concentrations. Pressures higher than 579 kPa produced excessive flow for both ink concentrations and did not yield discernibly different deposition mechanisms under the conditions considered. Similarly, three levels of nozzle-substrate distance (50 μm, 100 μm and 150 μm, namely, three integer multiples of the nozzle diameter) were considered. These distances were set by first contacting the nozzle on the substrate while observing it through the system microscope and prescribing the desired distance by moving the substrate down in the vertical direction. The printing speeds for different materials were experimentally determined such that continuous lines were formed under the aforementioned pressure and nozzle-substrate distance ranges. These speeds ranged from 1 to 25 mm/s. Each condition set is repeated 5 times for each material. Printing speed and distance parameters were randomized during the experiments since they can be automatically changed between each experiment.

During the experiments, two types of substrates, PDMS and acrylic, were used. PDMS is known for its low surface energy (low wettability) and elastic modulus compared to the acrylic. 30% inks were printed on both substrate types, whereas the 40% inks were printed only on the PDMS substrates. Circular acrylic substrates with 4 inch diameter were laser cut from commercially available Plexiglas sheets. PDMS substrates were prepared by casting two part platinum cured silicone (Slygard 184) into 4 inch circular petri dishes and curing them at room temperature for 24 hours followed by heat curing at 60ºC for an hour. During the initial step of the curing process, the petri dishes were kept on the printing system's motion platform to obtain flat surfaces for the experiments.

2.4. Analysis methods

Following the experimentation, cross-sectional profile of each line is measured using the laser profilometer. This profile is denoted by z(x) in Fig 2 (b) and is used to calculate the height (h) and width (w) of the line. The non-dimensional aspect ratio of the line is than calculated as $AR = h/w$. This profile is then used to estimate the average flow rate and the nozzle exit velocity (denoted by V_{avg} in Fig 2(a)). To this end, the cross-sectional area of the line is used to estimate the amount of ink deposited per unit line length which is multiplied by the printing speed and divided by the nozzle cross-sectional area:

$$V_{avg} = \frac{2f\int_{-w/2}^{w/2} z(x)dx}{c\pi R^2} \quad (1)$$

where R is the nozzle radius (25 μm) and c is the volumetric concentration of the inks. It should be noted that the final line profile is obtained following discernible water loss from the inks after they are deposited through evaporation. Accordingly, the estimated solid volume after evaporation should be divided by the volumetric concentration (c) of the ink to estimate the flow speed of the ink prior to evaporation. It has been shown for concentrated polymer solutions at room temperature, the volume additivity of the solvent and the solute is an accurate assumption [24]. As such, the volumetric concentration of the inks can be estimated by

$$c = \frac{\frac{N_{CMC}}{\rho_{CMC}}}{\frac{N_{CMC}}{\rho_{CMC}} + \frac{1-N_{CMC}}{\rho_{water}}} \quad (2)$$

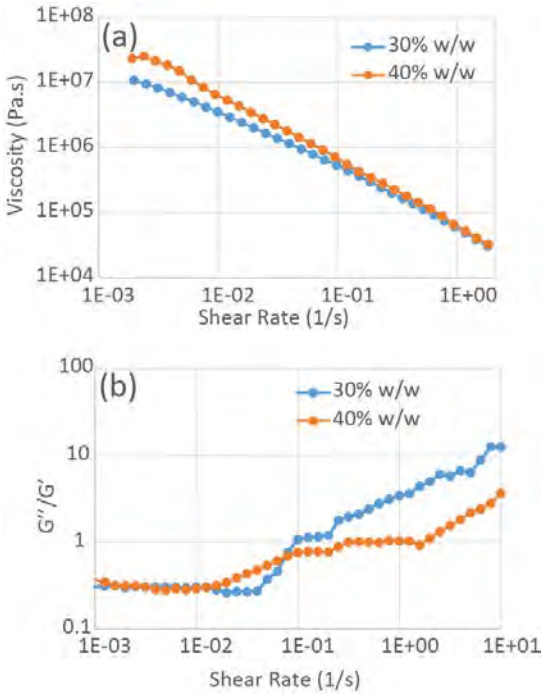

Fig. 3. (a) Result of the frequency sweep test, (b) Result of the amplitude sweep test

where N_{CMC} is the w/w concentration of the ink, ρ_{CMC}=1600 kg/m^3 is the density of pure CMC and ρ_{water}=1000 kg/m^3 is the density of water. Accordingly, the volumetric concentration of the 30% and 40% w/w inks were determined to be 21.9% and 29.4%, respectively. Having calculated the average flow velocity for each test, a non-dimensional velocity ratio is calculated as the $VR = V_{avg}/f$. As illustrated in Fig 2(c), a high velocity ratio greater than 1 is likely to produce bulging of the ink at the nozzle leading to excessive spreading and potential obstruction of the flow by the substrate. A low velocity ratio less than 1 leads to lagging of the printed ink filament behind the nozzle causing elongational stresses to form. As demonstrated in the author's earlier work, continuous deposition is not possible for inks with low elasticity in this case [17]. For elastic inks which can withstand the high elongational stresses, it has been shown that low velocity ratios leads to filament drawing effects, associated decrease in the nozzle exit pressure and elastocapillary thinning of the filaments, allowing high lateral resolution. In this work, we exclusively study the effect of velocity ratio on (1) the aspect ratio of the printed lines to understand the spreading effects and (2) flow velocity variation with respect to nozzle-substrate distance to explore the presence of flow obstruction or drawing effects.

Table 1. Maximum and minimum absolute dimensions of the printed lines .

Quantity	Value	Ink	Subst.	P (kPa)	f (mm/s)	d (μm)
Min Width (μm)	80.2	30%	Acrylic	193	5	100
	79.4	30%	PDMS	193	5	150
	57.5	40%	PDMS	193	10	100
Max Width (μm)	312.1	30%	Acrylic	579	1	100
	278.0	30%	PDMS	579	1	100
	304.8	40%	PDMS	579	5	50
Min Height (μm)	5.3	30%	Acrylic	193	5	50
	3.9	30%	PDMS	193	3	50
	7.1	40%	PDMS	193	12	50
Max Height (μm)	42.8	30%	Acrylic	579	4	50
	56.4	30%	PDMS	579	1	150
	63.8	40%	PDMS	579	2	150

3. Results and Discussions

3.1. Ink Rheology

Figure 3(a) presents the results of the frequency sweep test for both inks considered. As shown, both inks exhibit a shear thinning behavior which is a favorable property for DIW, facilitating ink flow under high shear stresses exhibited during deposition [14]. The 40% ink exhibits discernibly higher shear thinning consistent with the earlier findings for lower concentration aqueous CMC solutions [25]. The results of the amplitude sweep tests are given in Fig 3(b). Here, the vertical axis corresponds to the ratio between the viscous (G'') and elastic (G') moduli of the inks. A higher ratio simply indicates a more viscous fluid-like rather than elastic solid-like behavior at any given shear rate. As shown, the 30% ink showing a considerably more fluid-like behavior at higher shear rates, whereas the 40% ink clearly showing a more pronounced viscoelastic nature. For both inks, the modulus ratio is around 0.3<1 at low shear rates. This is also considered a favorable property for the DIW process [26], since it indicates that the deposited ink filament will "elastically resist" the flow and spreading, leading to high aspect ratio

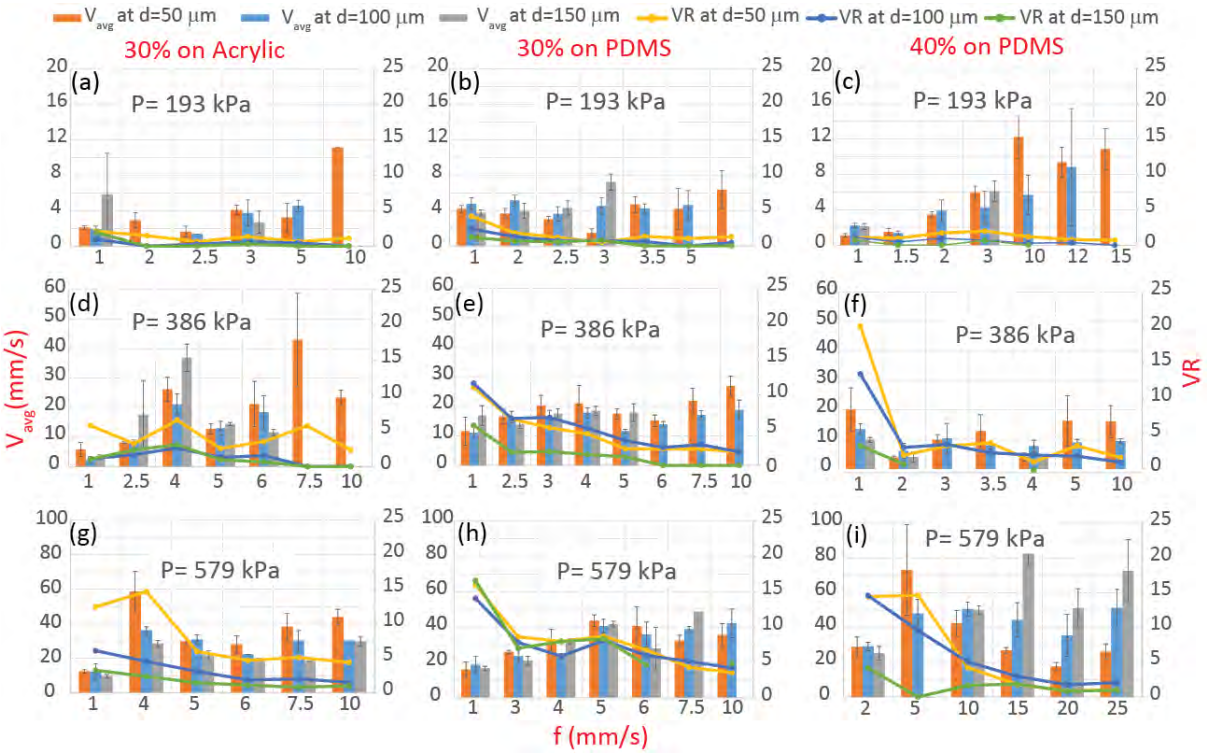

Fig. 4. Variation of average flow velocity and velocity ratio with printing speed and nozzle substrate distance at printing pressures of (a),(b) and (c) 193 kPa, (d), (e) and (f) 386 kPa, (g), (h) and (i) 579 kPa. Error bars represent the variation between five repetitions. An absent data point indicate that no continuous line was obtained for that set of parameters.

structures that can be stacked-up layer by layer.

3.2. DIW Experiments

Table 1 provides the noteworthy findings on the absolute geometries of the lines printed during the DIW experiments. The minimum line width were significantly higher than the nozzle diameter (50 µm) for the 30% ink unlike the 40% due to higher ink spreading after deposition. The highest amount of spreading was observed on the acrylic substrate as indicated by lowest maximum height and highest maximum width values recorded. The results presented in the later parts of the paper will primarily focus on the non-dimensional aspect ratios and their variation with the process parameters rather than the absolute quantities.

Figures 4 and 5 present the bar plots showing the average flow velocity (V_{avg}) and aspect ratio (AR) obtained through the DIW experiments, respectively. In the same plots, the velocity ratios for the same experiments are also presented (line plots) to identify data trends for various VR ranges and the associated deposition mechanisms.

Throughout the pressure ranges tested, continuous line printing was achieved at higher printing speeds (up to 25 mm/s) using the 40% ink compared to the 30% ink. This result, despite the fact that the 40% ink is more viscous and thus “harder to flow” at the same pressure, can be explained by the higher viscoelasticity of the 40% ink. Basically, the ink filaments can withstand higher extensional stresses at higher printing speeds leading to lower speed ratios.

It should be noted that without the influence of the substrate-material interactions, the flow rates and thus the average flow velocities are expected to stay constant under constant dispensing pressure and not be affected by the printing speed. As such the variations in a given plot in Figure 4 provide clues about how substrate-ink interactions affect the material flow. At the lowest tested pressure, the printing speed did not show a significant effect on the flow for the 30% ink. In same printing speed ranges, a discernible increase of the flow speed with printing speed was observed for the 40% ink (Fig 4(c)). Such an increase may indicate one of two phenomena: (1) the flow might be

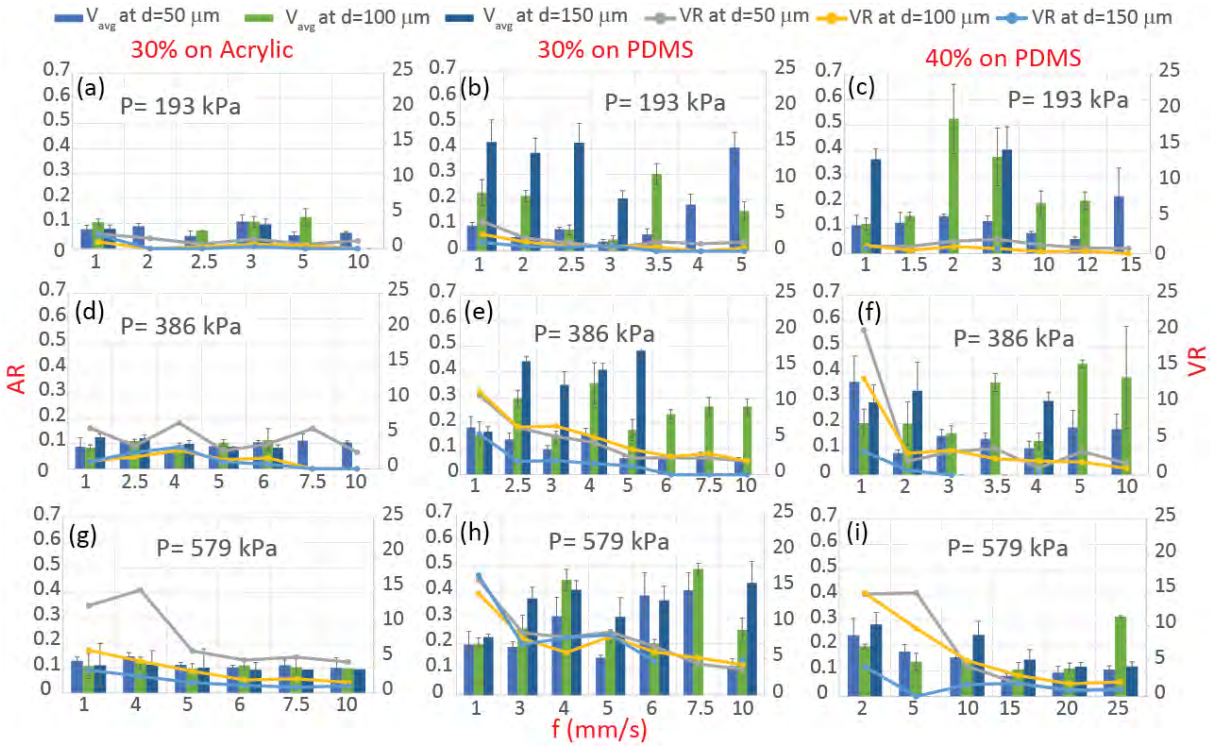

Fig. 5. Variation of aspect ratio and velocity ratio with printing speed and nozzle substrate distance at printing pressures of (a),(b) and (c) 193 kPa, (d), (e) and (f) 386 kPa, (g), (h) and (i) 579 kPa. Error bars represent the variation between five repetitions. An absent data point indicate that no continuous line was obtained for that set of parameters

obstructed by the substrate, an effect which would reduce with decreasing VR as the substrate moves faster to clear the deposited material away from the nozzle or (2) the deposition is dominated by the drawing mechanism and the substrate "pulls the filament out of the nozzle" faster. Given the VR values are only slightly above 1 for these experiments and the higher viscoelasticity of the 40% ink, the latter explanation is more suitable for the low pressures. At the higher pressures and low speeds for the 30% inks, a clear trend emerges as the flow velocities increase with increasing printing speed and settles around 20 mm/s for P=386 kPa and 40 mm/s for 579 kPa (Fig 4(e)-(h)). Considering the high VR values for the low speeds in these cases, it is likely that the flow obstruction is observed for VR>5 for the 30% inks. The nozzle-substrate distance (d) does not seem to affect the flow rate under these conditions. It has been shown in the literature that the flow rate-nozzle substrate distance correlation is observed when this distance is less than 50% of the nozzle diameter using newtonian inks [27]. In this study, minimum distance used is equal to the nozzle diameter, for which the substrate effect is unlikely.

As shown in Fig 5, the effect of the substrate on the final geometry is evident from the fact that consistently less than 0.1 aspect ratio is observed on the acrylic substrate. This is due to the high surface energy and elastic modulus of the acrylic substrate leading to excessive ink spreading. For the lines printed on the PDMS samples, aspect ratios up to 0.5 is obtained due to PDMS' low surface energy (hydrophobicity) leading to high wetting angles of the water based ink. In general, not a discernible difference between the 30 and 40% inks have been observed in terms of the aspect ratio. This can be explained by the similar modulus ratios of the inks at low shear rates as shown in Fig 2(b), leading to a similar spreading behavior under similar inertial and capillary forces following deposition. One distinct observation that can be made is generally increasing aspect ratios with increasing nozzle-substrate distance, particularly for the 30% ink on the PDMS substrate (Fig 5(b), (e) and (h)). This result indicates that the deposited material is compressed under the nozzle for

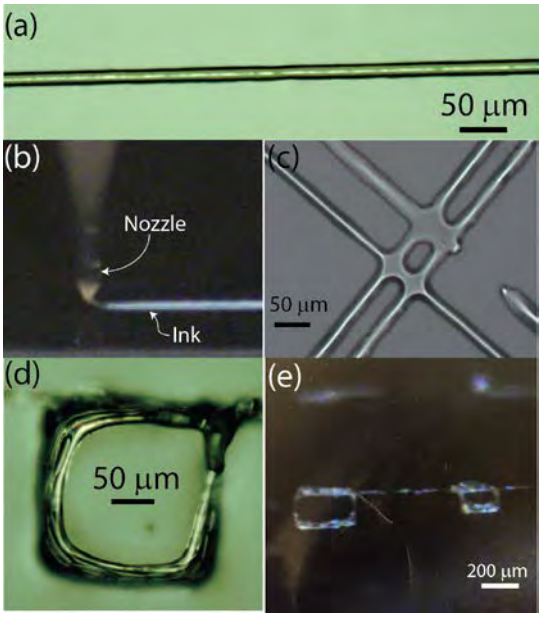

Fig.6.Results of the CMC DIW experiments using 10 and 30 μm diameter nozzles (a) 18 μm wide line obtained using a 30 μm nozzle and 45% w/w ink, (b) Deformation of the CMC ink filament during DIW, (c) Lines printed using 10 μm nozzle and 20% w/w ink, (d) and (e) Five layer square structures printed using 30 μm nozzle and 45% w/w ink

these experiments. This behavior is observed specifically for the high velocity ratios where flow obstruction was also observed. However, it is seen even for some cases where VR<5 and no apparent sign of flow rate reduction is noted (Fig 5(b)). For the lines printed on acrylic, no discernible variation with respect to printing speed or nozzle-substrate distance is noted. One can conclude that the capillary effects due to high surface energy dominate the spreading process for the acrylic surface rather than any mechanical effects coming from the nozzle-material interaction.

3.3. Preliminary observations on DIW with ultra-fine nozzles

For emerging applications of biodegradable polymers, there is a significant need for high fabrication resolution. For instance, for tissue engineering applications, the scaffolds fabricated using such polymers need to mimic the native tissue morphology which may show features <10 μm in size. The results presented above clearly shows that achieving in-plane feature sizes close to the nozzle diameter during DIW of similar materials is quite challenging and requires precise tuning of process parameters and proper substrates. Therefore, one can conclude that nozzles smaller than the desired resolution level should be used. Our preliminary results on the DIW with glass capillaries as small as 10 μm diameter is presented in Fig 6. Here, Fig 6(a) shows the 18 μm wide line printed with a nozzle having a diameter of 30 μm and a CMC concentration of 45% w/w. The line diameter being smaller than the nozzle diameter can be explained by the increased concentration of the ink leading to a more elastic behavior and associated elastocapillary thinning of the printed filaments. The stretching of the filament during the printing process is apparent in Fig 6(b). For the nozzle diameter of 10 μm, robust printing with CMC concentration above 20% w/w was not possible. This was primarily due to the fact that the high rate drying of the ink at the nozzle tip led to periodic clogging. At a concentration of 20% w/w, lines as small as 22 μm was achieved with these nozzles as shown in Fig 6(c). It should be noted that this line width is greater than what was obtained with a larger nozzle and higher concentration inks. This is due to increased spreading of the low concentration ink. This finding highlights an important constraint in DIW of these materials: Even though higher concentration inks are more desirable to obtain higher aspect ratio structures, they are not practical for low diameter nozzles. It's possible however, to utilize elastocapillary thinning to achieve smaller structures using larger nozzles, leading to an optimization problem. Finally, Fig 6 (d) and (e) demonstrates two 5-layer structures obtained using a 45% w/w ink, PDMS substrate and 30 μm nozzle. Under these conditions, the CMC ink exhibited ideal 3D stacking capability: a single layer line had a height of 8 μm and a five layer structure exhibited a height of 43 μm.

4. Conclusions

This paper presented the DIW process of degradable sodium CMC inks. In particular, the effect of ink concentration, substrate material and DIW process parameters on the printed structure geometry and flow characteristics are examined. It has been shown that the increased ink concentration led to higher viscoelastic behavior, especially at high shear rates experienced during deposition. This led to thinner lines and higher allowable speeds at low pressures. At higher pressures and low printing speeds, reduced flow rates were observed, indicating the influence of the substrate on the ink flow. On high

surface energy acrylic surfaces, the CMC inks exhibited excessive spreading and significantly lower aspect ratios compared to the PDMS surfaces. The nozzle-substrate distance has been shown to influence the aspect ratio of the printed structures, especially at high velocity ratios, indicating the mechanical compression of the printed material under these conditions. Finally, observations on printing of CMC inks using ultra-fine nozzles of 10 and 30 μm is presented. Features smaller than the nozzle size was printed utilizing the elastic properties of the high concentration inks at these sizes. Multi-layer three-dimensional structures were successfully fabricated.

The results of this study can be utilized to determine process and material parameters to achieve accurate fabrication of micro- and meso-scale CMC parts and structures. These findings also inform ink and process design for DIW of other biodegradable materials, contributing to emerging technologies such as artificial tissue engineering.

The future work will focus primarily on more comprehensive modeling and improvement of the process towards higher resolution. On the modelling side, we will follow this study up with a formal experimental study incorporating a wider range of material and process parameters and we will analyze the results through statistical tools such as ANOVA. This effort will reveal quantitative relationships between the process inputs and deposition mechanisms. In parallel, we will incorporate biodegradable inks in our ongoing efforts in computational modeling of the DIW process. This will involve complete shear and extensional rheological, capillary and thermal characterization of such inks and using these characteristics in a multi-physics model to predict the process outcomes. On the improvement front, we will focus our efforts in mitigating issues we face with high concentration inks when used with ultra-fine nozzles to obtain highly resolved printing with such inks.

Acknowledgements

The authors would like to acknowledge the funding from National Science Foundation (NSF) awards 1658845 and 1606226,

References

[1] W. Amass, A. Amass, B. Tighe, A review of biodegradable polymers: uses, current developments in the synthesis and characterization of biodegradable polyesters, blends of biodegradable polymers and recent advances in biodegradation studies Polym. Int. 47 (1998) 89–144.

[2] H. Tian, Z. Tang, X. Zhuang, X. Chen, X. Jing, Prog. Biodegradable synthetic polymers: Preparation, functionalization and biomedical application Polym. Sci. 37 (2012) 237–280.

[3] C.K. Chua, K.F. Leong, K.H. Tan, F.E. Wiria, C.M. Cheah, Development of tissue scaffolds using selective laser sintering of polyvinyl alcohol/hydroxyapatite biocomposite for craniofacial and joint defects J. Mater. Sci. Mater. Med. 15 (2004) 1113–1121.

[4] J.M. Williams, A. Adewunmi, R.M. Schek, C.L. Flanagan, P.H. Krebsbach, S.E. Feinberg, S.J. Hollister, S. Das, Bone tissue engineering using polycaprolactone scaffolds fabricated via selective laser sintering Biomaterials 26 (2005) 4817–4827.

[5] S.S. Kim, H. Utsunomiya, J.A. Koski, B.M. Wu, M.J. Cima, J. Sohn, K. Mukai, L.G. Griffith, J.P. Vacanti, Survival and Function of Hepatocytes on a Novel Three-Dimensional Synthetic Biodegradable Polymer Scaffold With an Intrinsic Network of Channels Ann. Surg. 228 (1998) 8–13.

[6] F.P.W. Melchels, J. Feijen, D.W. Grijpma, A review on stereolithography and its applications in biomedical engineering Biomaterials 31 (2010) 6121–6130.

[7] S.J. Kalita, S. Bose, H.L. Hosick, A. Bandyopadhyay, Development of controlled porosity polymer-ceramic composite scaffolds via fused deposition modeling Mater. Sci. Eng. C 23 (2003) 611–620.

[8] W. Schuurman, P. a. Levett, M.W. Pot, P.R. van Weeren, W.J. a Dhert, D.W. Hutmacher, F.P.W. Melchels, T.J. Klein, J. Malda, Gelatin-methacrylamide hydrogels as potential biomaterials for fabrication of tissue-engineered cartilage constructs Macromol. Biosci. 13 (2013) 551–561.

[9] H.N. Chia, B.M. Wu, Recent advances in 3D printing of biomaterials J. Biol. Eng. 9 (2015) 4.

[10] Ozbolat IT, Hospodiuk M. Current advances and future perspectives in extrusion-based bioprinting. Biomaterials 2016;76:321–43.

[11] J. Russias, E. Saiz, S. Deville, K. Gryn, G. Liu, R.K. Nalla, A.P. Tomsia, Fabrication and in vitro characterization of three-dimensional organic / inorganic scaffolds by robocasting M.S. Division, L. Berkeley, (2007).

[12] W. Schuurman, V. Khristov, M.W. Pot, P.R. van Weeren, W.J. a Dhert, J. Malda, Bioprinting of hybrid tissue constructs with tailorable mechanical properties Biofabrication 3 (2011) 021001.

[13] J. Kundu, J.H. Shim, J. Jang, S.W. Kim, D.W. Cho, An additive manufacturing-based PCL-alginate-chondrocyte bioprinted scaffold for cartilage tissue engineering J. Tissue Eng. Regen. Med. (2013).

[14] J. a. Lewis, Direct Ink Writing of 3D Functional Materials Adv. Funct. Mater. 16 (2006) 2193–2204.

[15] J.T. Muth, D.M. Vogt, R.L. Truby, Y. Mengüç, D.B. Kolesky, R.J. Wood, J. a. Lewis, Embedded 3D Printing of Strain Sensors within Highly Stretchable Elastomers Adv. Mater. (2014) n/a–n/a.

[16] M. Noman Hasan, M. Vatani, A. Chandy, J.-W. Choi Experimental and Numerical Analysis of Filament Front Deformation for Direct-Print, J. Manuf. Sci. Eng. 138 (2016) 011003.

[17] S. Nesaei, M.D. Rock, Y. Wang, M. Kessler, A. Gozen, Additive Manufacturing with Conductive, Viscoelastic Polymer Composites: Direct-Ink-Writing of Electrolytic and Anodic Poly(ethylene oxide) Composites J. Manuf. Sci. Eng. 139 (2017) 1–52.

[18] N.E. Fedorovich, I. Swennen, J. Girones, L. Moroni, C. a van Blitterswijk, E. Schacht, J. Alblas, W.J. a Dhert, Evaluation of photocrosslinked Lutrol hydrogel for tissue printing applications. Biomacromolecules 10 (2009) 1689–96.

[19] L.G. Bracaglia, B.T. Smith, E. Watson, N. Arumugasaamy, A.G. Mikos, J.P. Fisher, 3D printing for the design and fabrication of polymer-based gradient scaffolds Acta Biomater. 56 (2017) 3–13.

[20] Y.-C. Yeh, C.B. Highley, L. Ouyang, J.A. Burdick, 3D printing of photocurable poly(glycerol sebacate) elastomers Biofabrication 8 (2016) 045004.

[21] Y. Bao, J. Ma, N. Li, Synthesis and swelling behaviors of sodium carboxymethyl cellulose-g-poly(AA-co-AM-co-AMPS)/MMT superabsorbent hydrogel Carbohydr. Polym. 84 (2011) 76–82.

[22] B. Bediz, E. Korkmaz, R. Khilwani, C. Donahue, G. Erdos, L.D. Falo, O.B. Ozdoganlar, Dissolvable microneedle arrays for intradermal delivery of biologics: Fabrication and application Pharm. Res. 31 (2014) 117–135.

[23] Korkmaz, E., Friedrich, E. E., Ramadan, M. H., Erdos, G., Mathers, A. R., Ozdoganlar, O. B., ... & Falo Jr, L. D. (2015). Therapeutic intradermal delivery of tumor necrosis factor-alpha antibodies using tip-loaded dissolvable microneedle arrays. Acta biomaterialia, 24, 96-105.

[24] R.D.C. Cruz, R.J. Martins, M.J.E.D.M. Cardoso, O.E. Barcia, Volumetric study of aqueous solutions of polyethylene glycol as a function of the polymer molar mass in the temperature range 283.15 to 313.15 K and 0.1 MPa J. Solution Chem. 38 (2009) 957–981.

[25] M. Edali, M.N. Esmail, G.H. Vatistas, Rheological properties of high concentrations of carboxymethyl cellulose solutions J. Appl. Polym. Sci. 79 (2001) 1787–1801.

[26] J. Lewis, G. Gratson, Direct writing in three dimensions Mater. Today (2004) 32–39.

[27] B. Li, P. a Clark, K.H. Church, Robust Direct-Write Dispensing Tool and Solutions for Micro/Meso-Scale Manufacturing and Packaging ASME_IEEE Int. Manuf. Sci. Eng. Conf. (2007) 1–7.